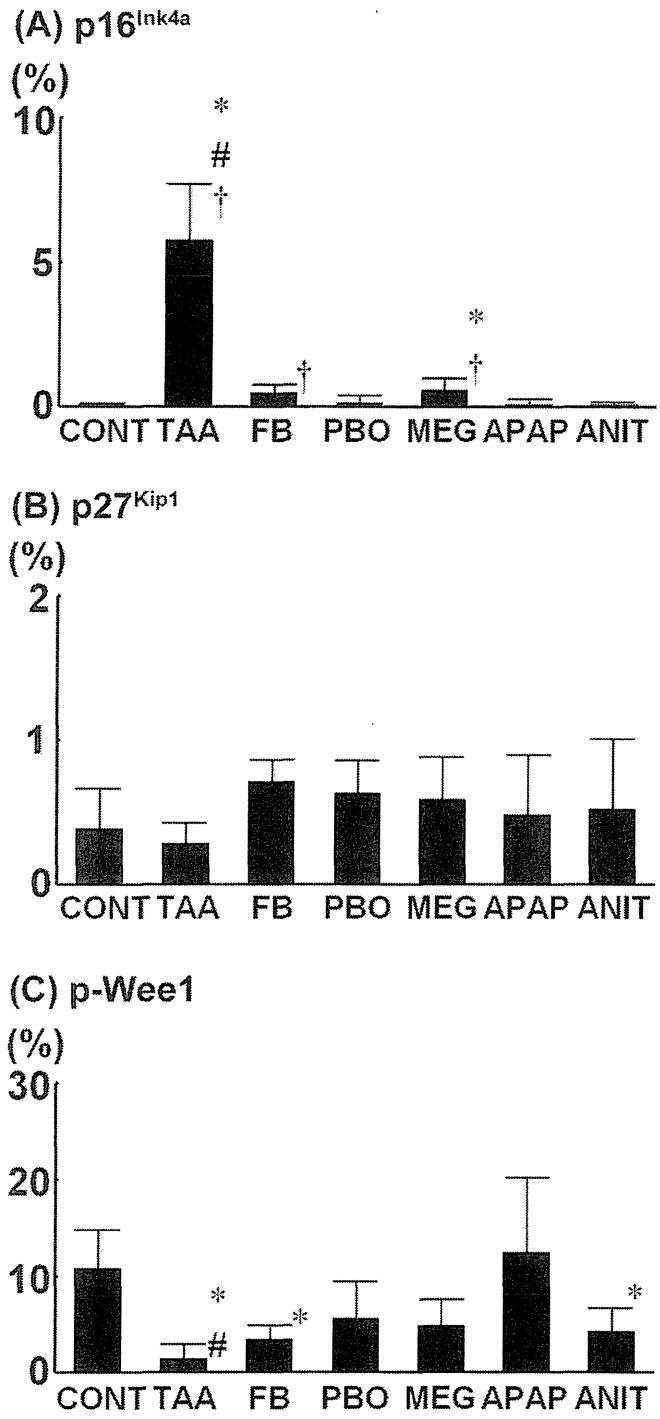

Fig. 8. Immunohistochemical cellular distribution of $p16^{Ink4a}$, $p27^{Kip1}$, and p-Wee1 in the initial screening in liver cells after 28-day treatment with hepatocarcinogens or non-carcinogens in rats. The graphs show positive cell ratios (%) of liver cells per total cells counted using five animals in each group. Values are presented as mean + SD. (A) $p16^{Ink4a}$, (B) $p27^{Kip1}$ and (C) p-Wee1. * $P < 0.05$ vs. untreated controls (Dunnett's or Steel's test). $^{\#}$ $P < 0.05$ vs. APAP (Dunnett's or Steel's test). † $P < 0.05$ vs. ANIT (Dunnett's or Steel's test).

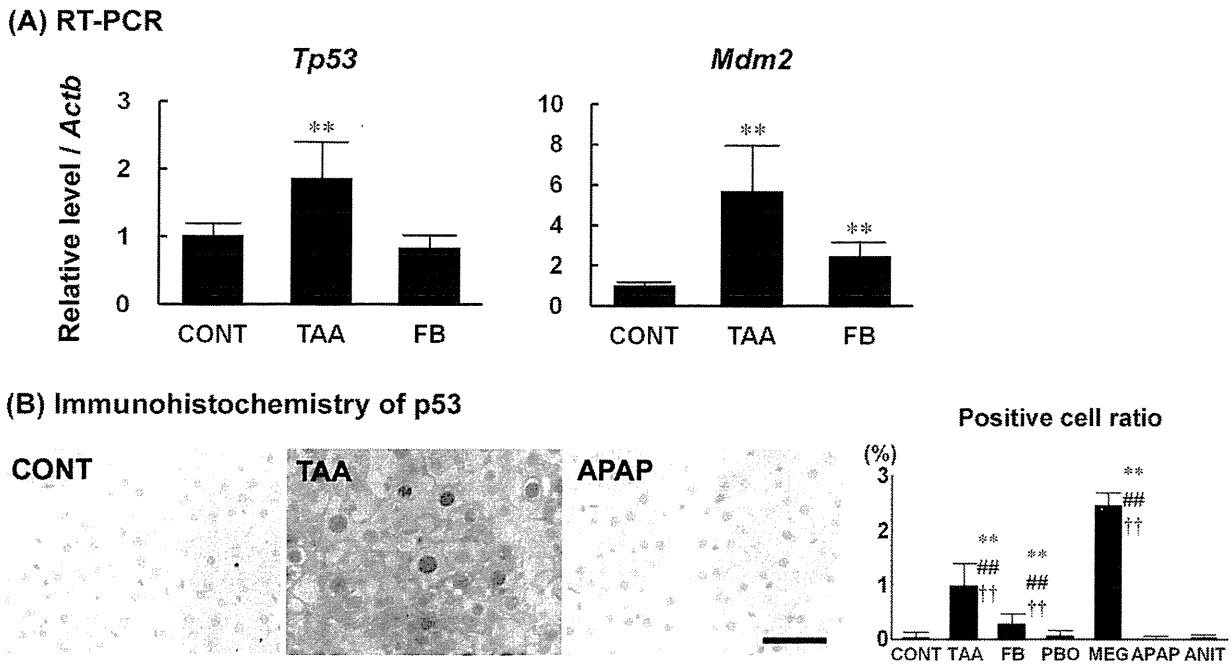

Fig. 9. Expression of p53 and downstream Mdm2 in the liver after 28-day treatment with hepatocarcinogens in rats. (A) Real-time RT-PCR analysis of p53 and Mdm2. Values are expressed as group mean fold changes over untreated controls. Values represent mean + SD *,** $P < 0.05$, 0.01 vs. untreated controls (Dunnett's or Steel's test). (B) Immunohistochemical cellular distribution of p53 in liver cells. Photomicrographs show immunoreactive cell distributions of p53 in the liver cells in representative cases of an untreated control and animals treated with TAA or APAP. The graphs show positive cell ratios (%) of liver cells per total cells counted using 10 animals in each group. Magnification: ×400 (Bar = 50 μm). *,** $P < 0.05$, 0.01 vs. untreated controls (Dunnett's or Steel's test). $^{\#,\#\#}$ $P < 0.05$, 0.01 vs. APAP (Dunnett's or Steel's test). †,††: $P < 0.05$, 0.01 vs. ANIT (Dunnett's or Steel's test).

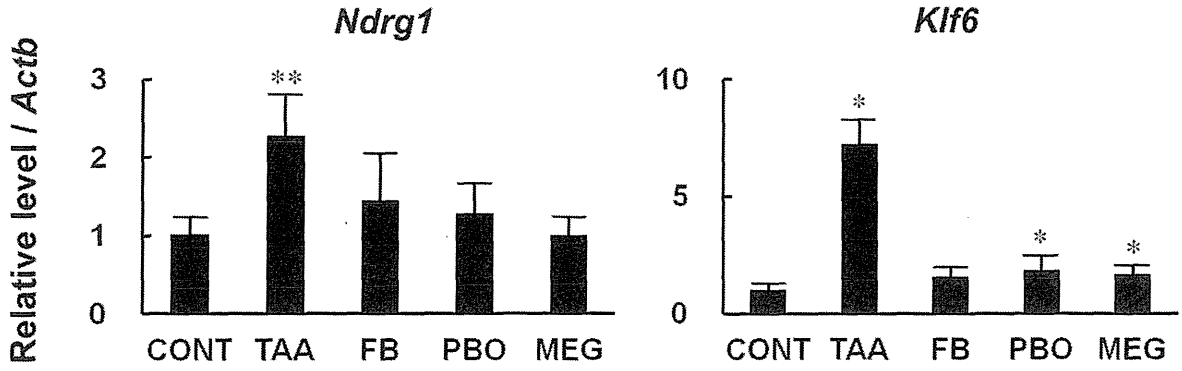

Fig. 10. Real-time RT-PCR analysis of Ndrg1 and Klf6. Values are expressed as group mean fold changes over untreated controls. Numbers of animals examined were 6 in each group. Values represent mean + SD *, ** $P < 0.05$, 0.01 vs. untreated controls (Dunnett's or Steel's test).

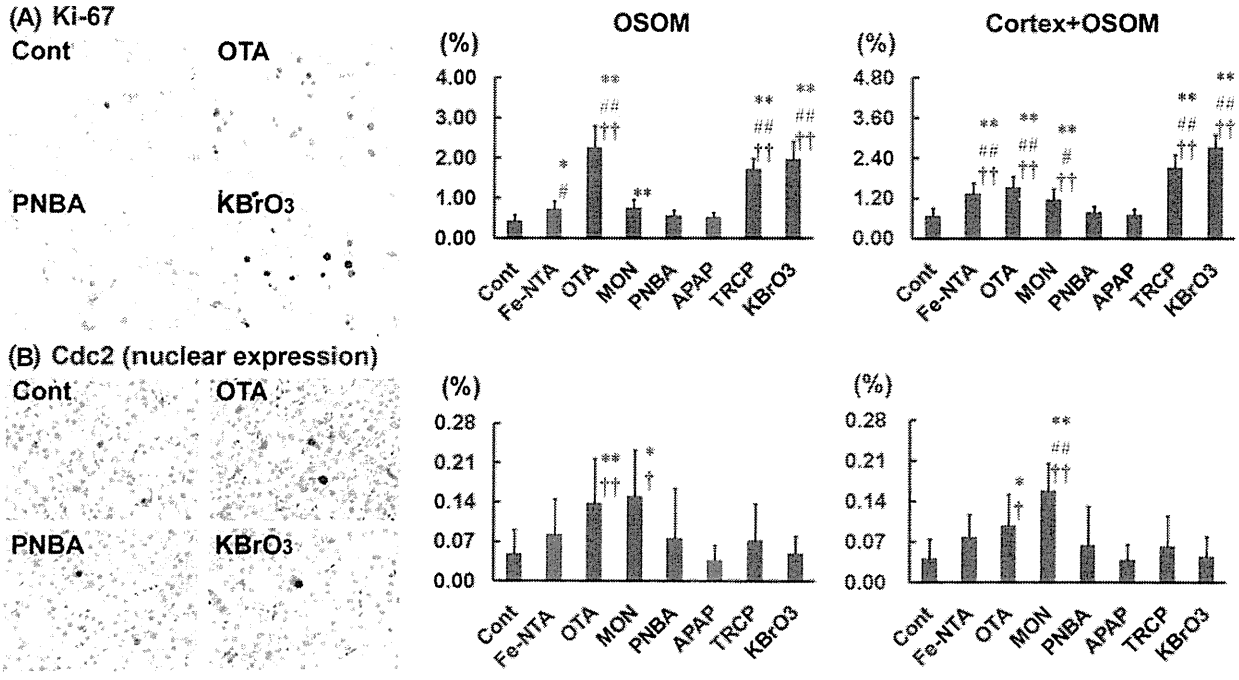

Fig. 11. Immunohistochemical cellular distribution of Ki-67 and Cdc2 selected from the initial screening in the renal tubular epithelia after 28-day treatment with renal carcinogens or non-carcinogens in rats. Photomicrographs show immunoreactive cell distributions of Ki-67 and nuclear Cdc2 in the OSOM in representative cases of untreated controls and animals treated with OTA, PNBA, and KBrO3. The graphs show positive cell ratios (%) of proximal tubular epithelial cells per total cells counted in the OSOM (left) and cortex + OSOM (right) using 10 animals in each group. (A) Ki-67 and (B) nuclear Cdc2. *,** $P < 0.05$, 0.01 versus untreated controls (Dunnett's or Steel's test). $^{\#,\#\#}$ $P < 0.05$, 0.01 versus PNBA (Dunnett's or Steel's test). †,†† $P < 0.05$, 0.01 versus APAP (Dunnett's or Steel's test)

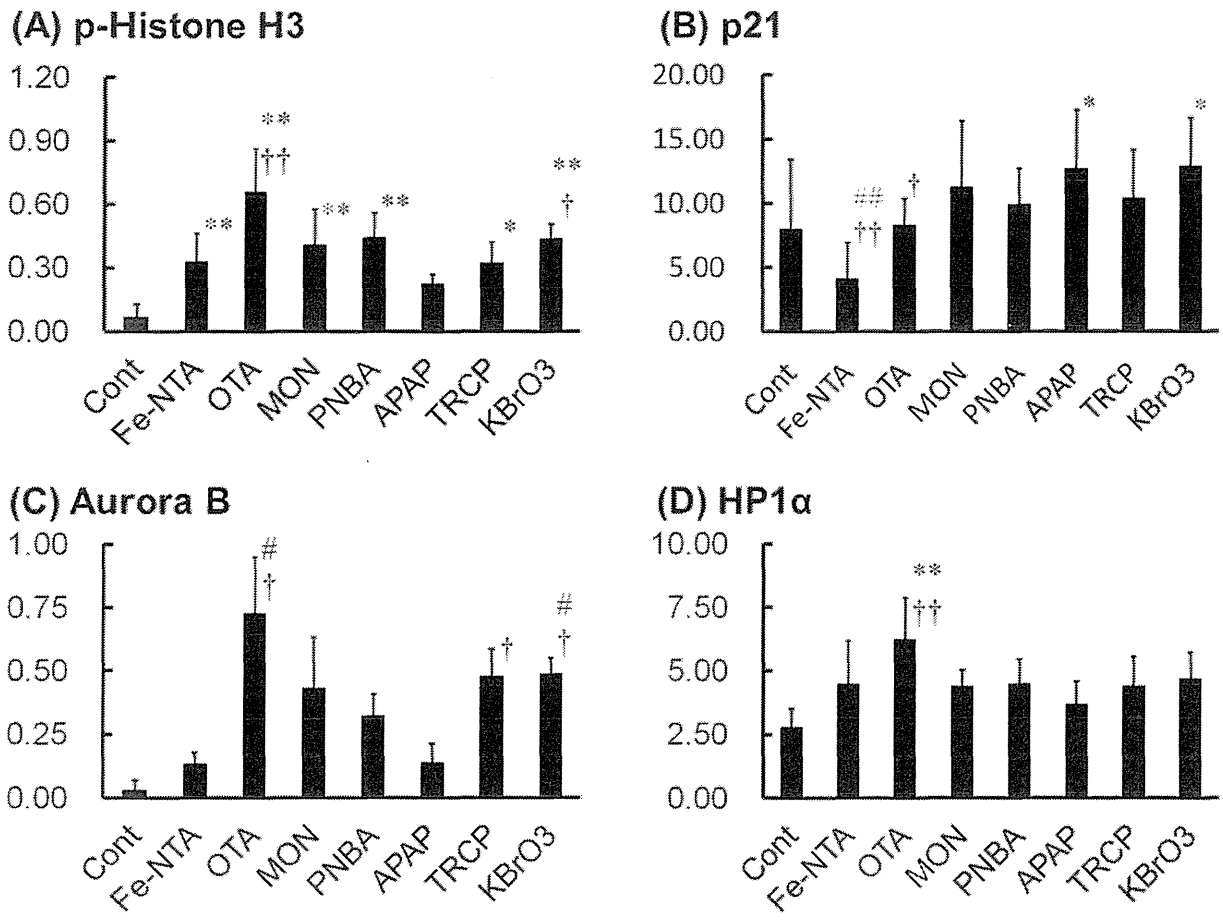

Fig. 12. Immunohistochemical cellular distribution of cell cycle-related molecules in the initial screening of the OSOM after after 28-day treatment with renal carcinogens or non-carcinogens in rats. The graphs show positive cell ratios (%) of proximal tubular epithelial cells per total cells counted in the OSOM of molecules in the initial screening using five animals from each group. Values are presented as mean + SD. (A) p-Histone H3, (B) $p21^{Cip1}$, (C) Aurora B and (D) HP1α. *,** $P < 0.05$, 0.01 versus untreated controls (Dunnett's or Steel's test). $^{\#,\#\#}$ $P < 0.05$, 0.01 versus PNBA (Dunnett's or Steel's test). †,†† $P < 0.05$, 0.01 versus APAP (Dunnett's or Steel's test).

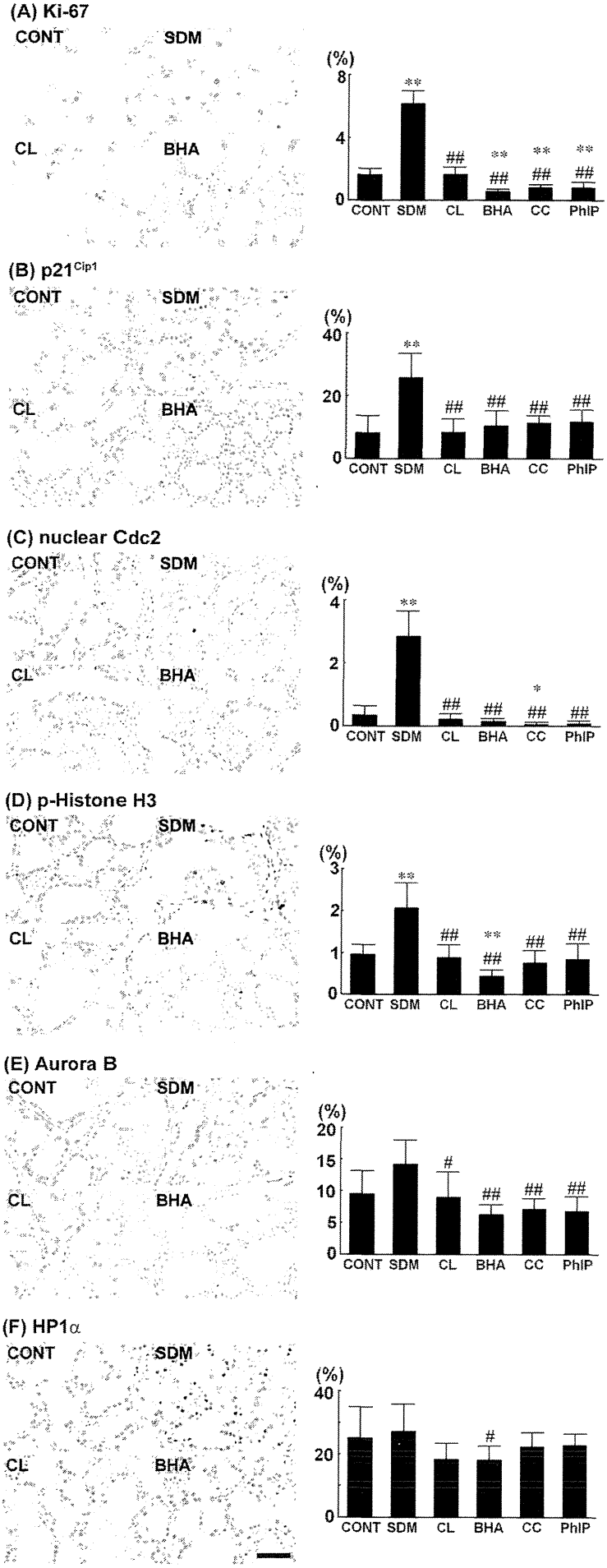

Fig. 13. Distribution of Ki-67^{+}, p21^{Cip1+}, nuclear Cdc2^{+}, p-Histone H3^{+}, Aurora B^{+} and HP1α^{+} cells in the thyroid. Photomicrographs show Ki-67^{+}, p21^{Cip1+}, nuclear Cdc2^{+}, p-Histone H3^{+}, Aurora B^{+} and HP1α^{+} cells in untreated controls and animals treated with SDM, CL or BHA. The graphs show positive cell ratios (%) of epithelial cells per total cells counted in each target organ using 10 animals per group. Values represent mean + SD. (A) Ki-67, (B) p21^{Cip1}, (C) nuclear Cdc2, (D) p-Histone H3, (E) Aurora B and (F) HP1α. Bar = 50 μm. *,** $P < 0.0056$, 0.0011 vs. untreated controls (Student's *t*-test with Bonferroni correction). $^{\#,\#\#}$ $P < 0.0056$, 0.0011 vs. SDM (Student's *t*-test with Bonferroni correction).

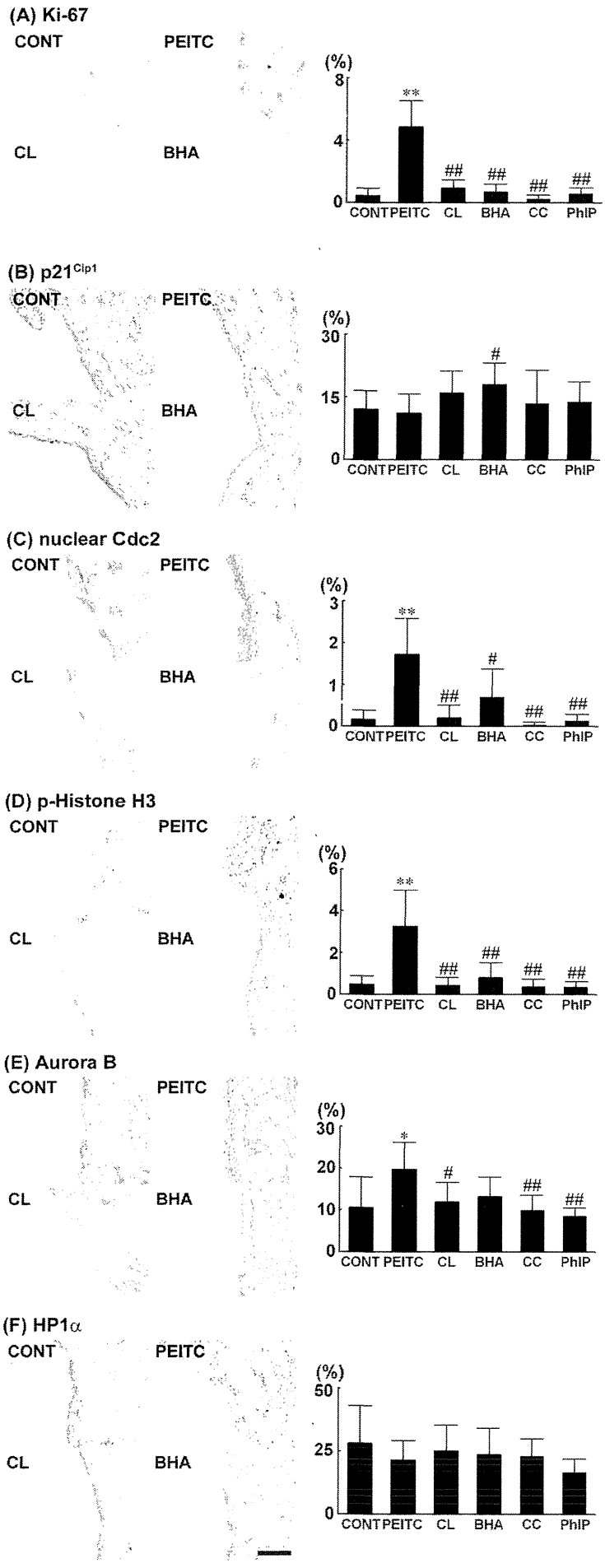

Fig. 14. Distribution of Ki-67^{+}, p21^{Cip1+}, nuclear Cdc2^{+}, p-Histone H3^{+}, Aurora B^{+} and HP1α^{+} cells in the urinary bladder. Photomicrographs show Ki-67^{+}, p21^{Cip1+}, nuclear Cdc2^{+}, p-Histone H3^{+}, Aurora B^{+} and HP1α^{+} cells in untreated controls and animals treated with PEITC, CL or BHA. The graphs show positive cell ratios (%) of epithelial cells per total cells counted in each target organ using 10 animals per group. Values represent mean + SD. (A) Ki-67, (B) p21^{Cip1}, (C) nuclear Cdc2, (D) p-Histone H3, (E) Aurora B and (F) HP1α. Bar = 100 μm. *,** $P < 0.0056$, 0.0011 vs. untreated controls (Student's *t*-test with Bonferroni correction). $^{\#,\#\#}$ $P < 0.0056$, 0.0011 vs. PEITC (Student's *t*-test with Bonferroni correction).

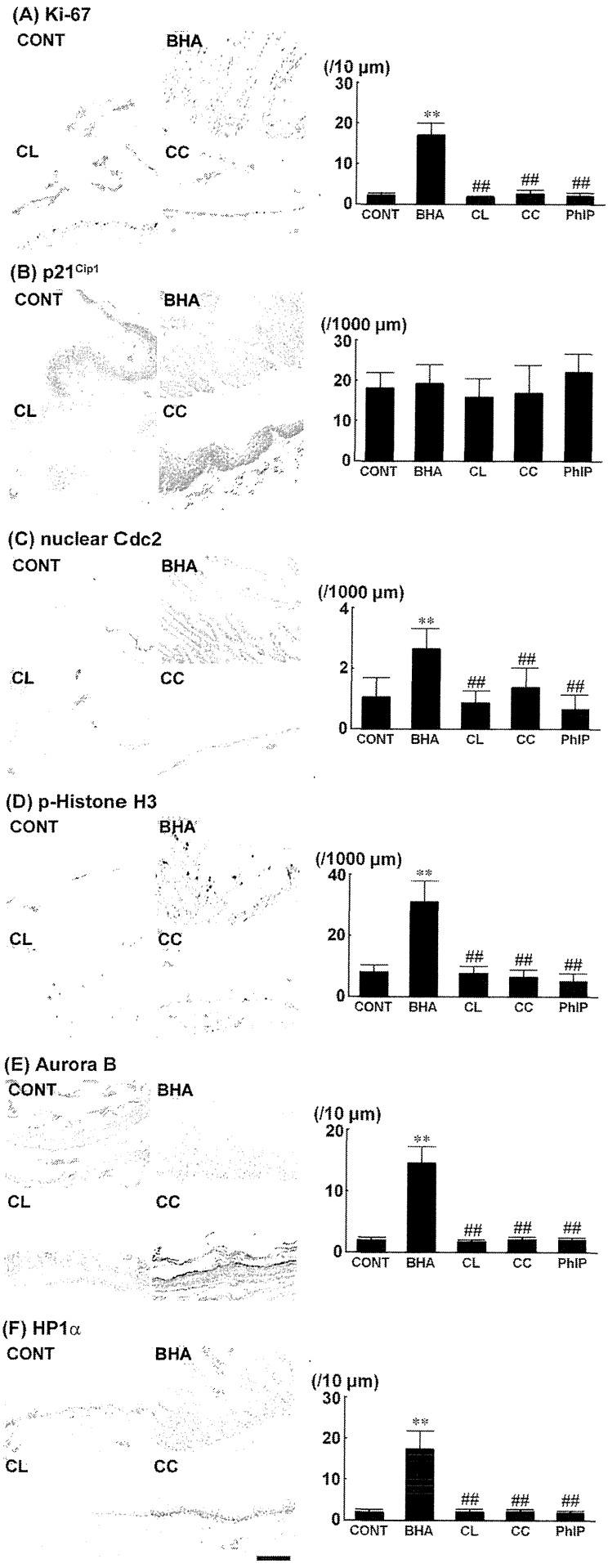

Fig. 15. Distribution of Ki-67^{+}, p21^{Cip1+}, nuclear Cdc2^{+}, p-Histone H3^{+}, Aurora B^{+} and HP1α^{+} cells in the forestomach. Photomicrographs show Ki-67^{+}, p21^{Cip1+}, nuclear Cdc2^{+}, p-Histone H3^{+}, Aurora B^{+} and HP1α^{+} cells in untreated controls and animals treated with BHA, CL or CC. (A), (E) and (F) show vertical length of positive cell distribution from the basement membrane per unit area using 10 animals per group. (B), (C) and (D) show mean number of positive cells per unit horizontal length (1,000 μm). Values represent mean + SD. (A) Ki-67, (B) p21^{Cip1}, (C) nuclear Cdc2, (D) p-Histone H3, (E) Aurora B and (F) HP1α. Bar = 100 μm. ** $P < 0.0014$ vs. untreated controls (Student's *t*-test with Bonferroni correction). $^{\#\#}$ $P < 0.0014$ vs. BHA (Student's *t*-test with Bonferroni correction).

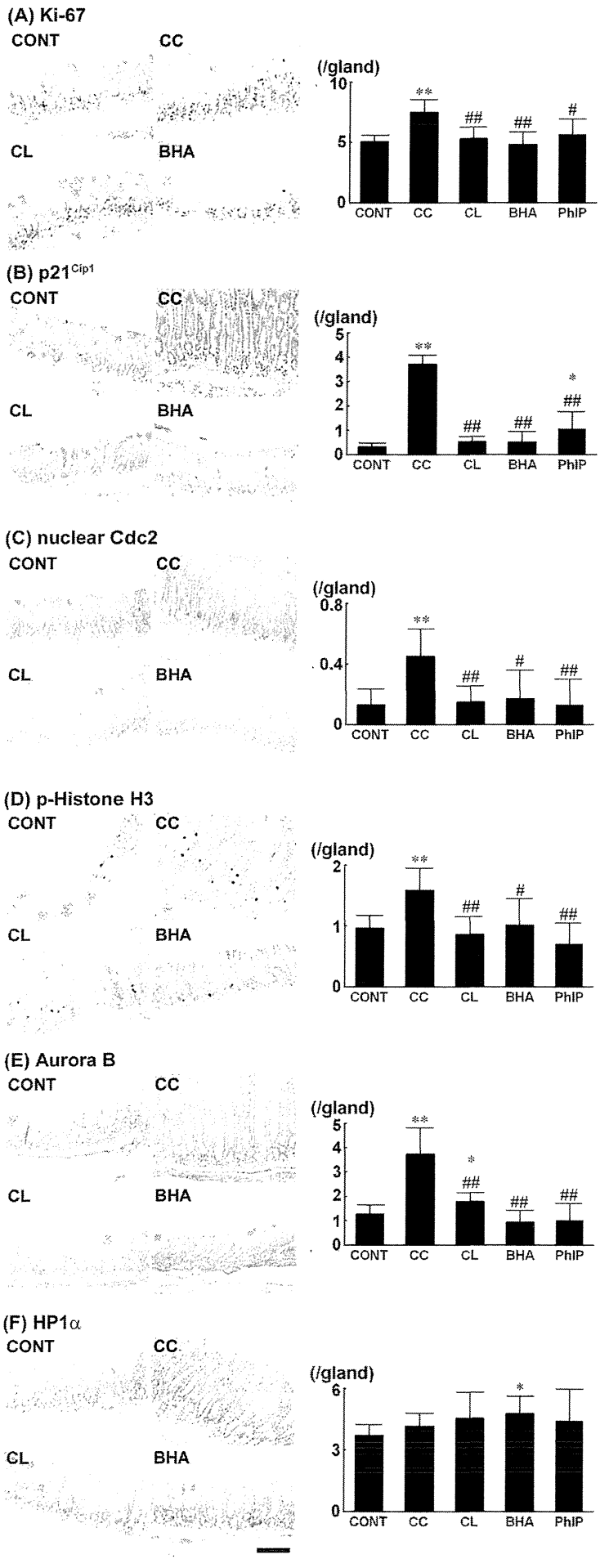

Fig. 16. Distribution of Ki-67^{+}, p21^{Cip1+}, nuclear Cdc2^{+}, p-Histone H3^{+}, Aurora B^{+} and HP1α^{+} cells in the glandular stomach. Photomicrographs show Ki-67^{+}, p21^{Cip1+}, nuclear Cdc2^{+}, p-Histone H3^{+}, Aurora B^{+} and HP1α^{+} cells in untreated controls and animals treated with CC, CL or BHA. The graphs show mean number of positive cells per gland using 10 animals per group. Values represent mean + SD. (A) Ki-67, (B) p21^{Cip1}, (C) nuclear Cdc2, (D) p-Histone H3, (E) Aurora B and (F) HP1α. Bar = 100 μm. *,** $P < 0.0071$, 0.0014 vs. untreated controls (Student's *t*-test with Bonferroni correction). $^{\#,\#\#}$ $P < 0.0071$, 0.0014 vs. CC (Student's *t*-test with Bonferroni correction).

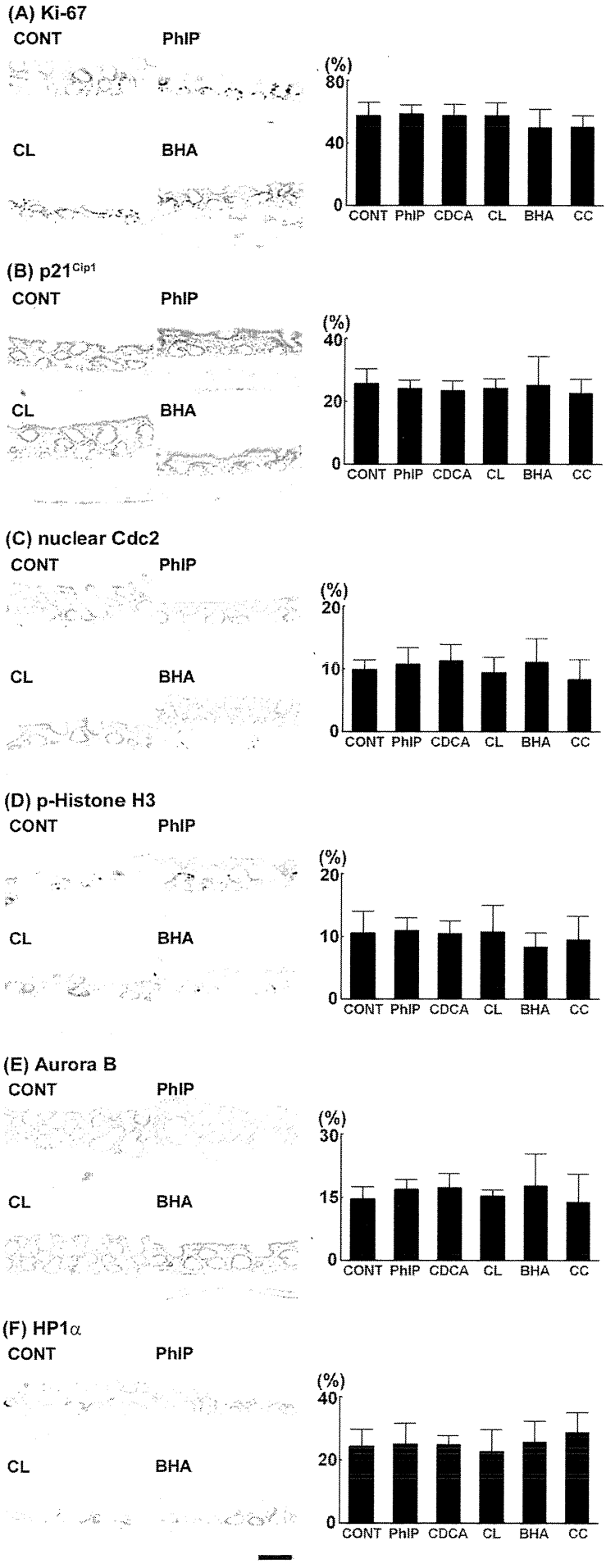

Fig. 17. Distribution of Ki-67^{+}, p21^{Cip1+}, nuclear Cdc2^{+}, p-Histone H3^{+}, Aurora B^{+} and HP1α^{+} cells in the colon. Photomicrographs show Ki-67^{+}, p21^{Cip1+}, nuclear Cdc2^{+}, p-Histone H3^{+}, Aurora B^{+} and HP1α^{+} cells in the colon in untreated controls and animals treated with PhIP, CL or BHA. The graphs show positive cell ratios (%) of epithelial cells per total cells counted in crypts using 10 animals per group. Values represent mean + SD. (A) Ki-67, (B) p21^{Cip1}, (C) nuclear Cdc2, (D) p-Histone H3, (E) Aurora B and (F) HP1α. Bar = 100 μm.

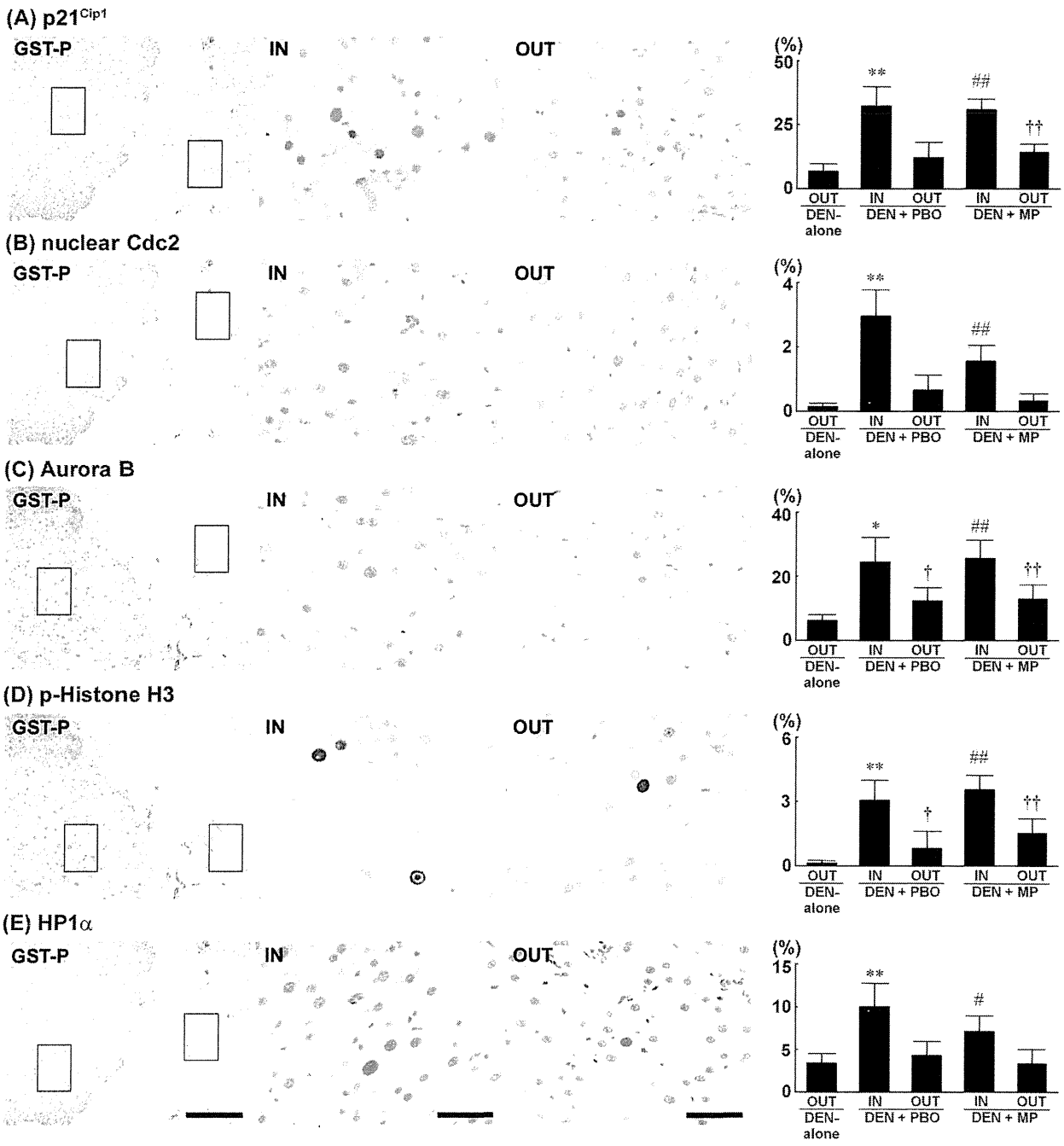

Fig. 18. Distribution of Ki-67^{+}, p21^{Cip1+}, nuclear Cdc2^{+}, Aurora B^{+}, p-Histone H3^{+} and HP1α^{+} cells in early hepatocarcinogenesis. Photomicrographs show the cellular distributions of markers inside and outside the GST-P^{+} foci in the DEN + PBO group. The graphs show positive cell ratios (%) of liver cells inside (IN) and outside (OUT) the GST-P^{+} foci in the DEN + PBO and DEN + MP groups, and the outside the GST-P^{+} foci in the DEN-alone group. Values represent mean + SD. (A) Ki-67, (B) p21^{Cip1}, (C) nuclear Cdc2, (D) Aurora B, (E) p-Histone H3, and (F) HP1α. Bar = 200 μm (GST-P), Bar = 50 μm (IN, OUT). *, ** $P < 0.05$, 0.01 vs. OUT in the DEN + PBO group (Tukey's or Steel-Dwass multiple comparison test). $^{\#}$, $^{\#\#}$ $P < 0.05$, 0.01 vs. OUT in the DEN + MP group (Tukey's or Steel-Dwass multiple comparison test). †, †† $P < 0.05$, 0.01 vs. OUT in the DEN-alone group (Tukey's or Steel-Dwass multiple comparison test).

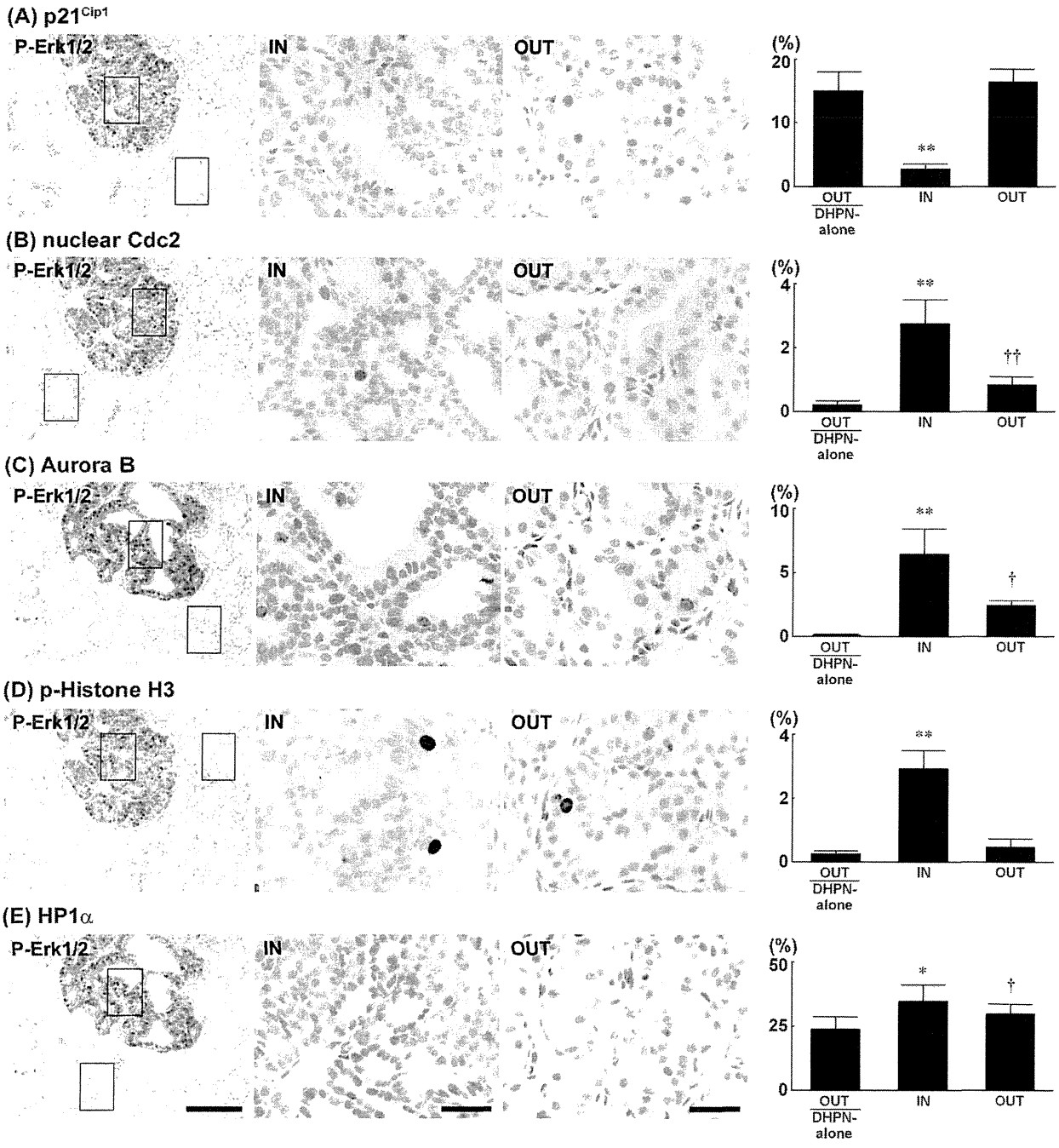

Fig. 19. Distribution of Ki-67^{+}, p21^{Cip1+}, nuclear Cdc2^{+}, Aurora B^{+}, p-Histone H3^{+} and HP1α^{+} cells in early thyroid carcinogenesis. Photomicrographs show the cellular distributions of markers inside or outside the p-Erk1/2^{+} FFCHs in the DHPN + SDM group. The graphs show positive cell ratios (%) of thyroid follicular cells inside (IN) or outside (OUT) the p-Erk1/2^{+} FFCHs in the DHPN + SDM group, and the outside the p-Erk1/2^{+} FFCHs in the DHPN-alone group. Values represent mean + SD. (A) Ki-67, (B) p21^{Cip1}, (C) nuclear Cdc2, (D) Aurora B, (E) p-Histone H3, and (F) HP1α. Bar = 100 μm (p-Erk1/2), Bar = 30 μm (IN, OUT). *,** $P < 0.05$, 0.01 vs. OUT in the DHPN + SDM group (Tukey's or Steel-Dwass multiple comparison test). †,†† $P < 0.05$, 0.01 vs. OUT in the DHPN-alone group (Tukey's or Steel-Dwass multiple comparison test).

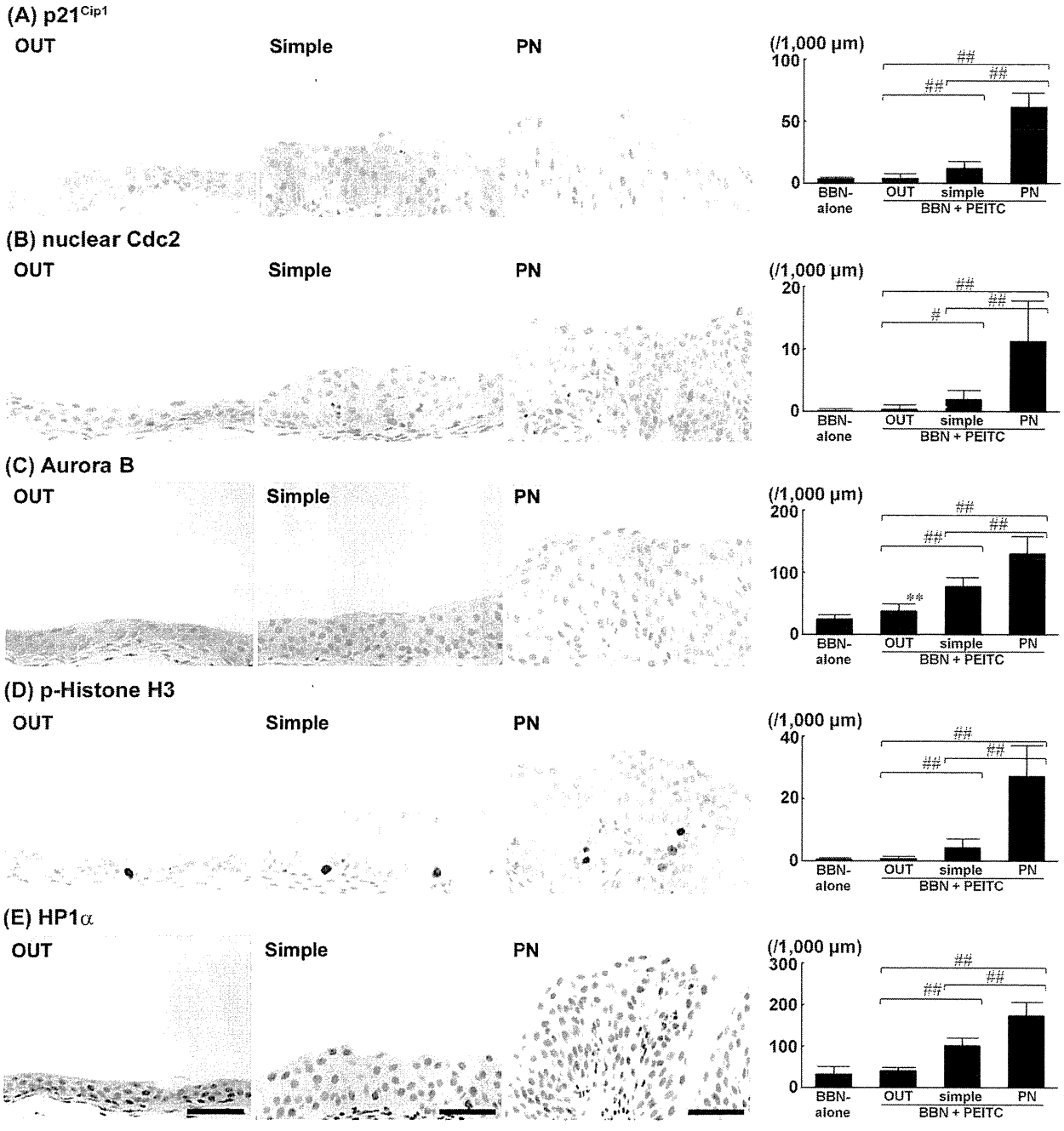

Fig. 20. Distribution of Ki-67^{+}, p21^{Cip1+}, nuclear Cdc2^{+}, Aurora B^{+}, p-Histone H3^{+} and HP1α^{+} cells in early urinary bladder carcinogenesis. Photomicrographs show the cellular distributions of markers in simple hyperplastic foci, PN hyperplastic foci and surrounding epithelial cells in the BBN + PEITC group. The graphs show positive cells per unit muscularis mucosae length (1,000 μm) of the urothelium in the BBN-alone group, and of surrounding urothelium (OUT), and simple or PN hyperplastic foci in the BBN + PEITC group. Values represent mean + SD. (A) Ki-67, (B) p21^{Cip1}, (C) nuclear Cdc2, (D) Aurora B, (E) p-Histone H3, and (F) HP1α. Bar = 50 μm. ** $P < 0.01$ vs. the BBN-alone group (Tukey's or Steel-Dwass multiple comparison test). $^{\#,\#\#}$ $P < 0.05$, 0.01 between the groups for comparison (Tukey's or Steel-Dwass multiple comparison test).

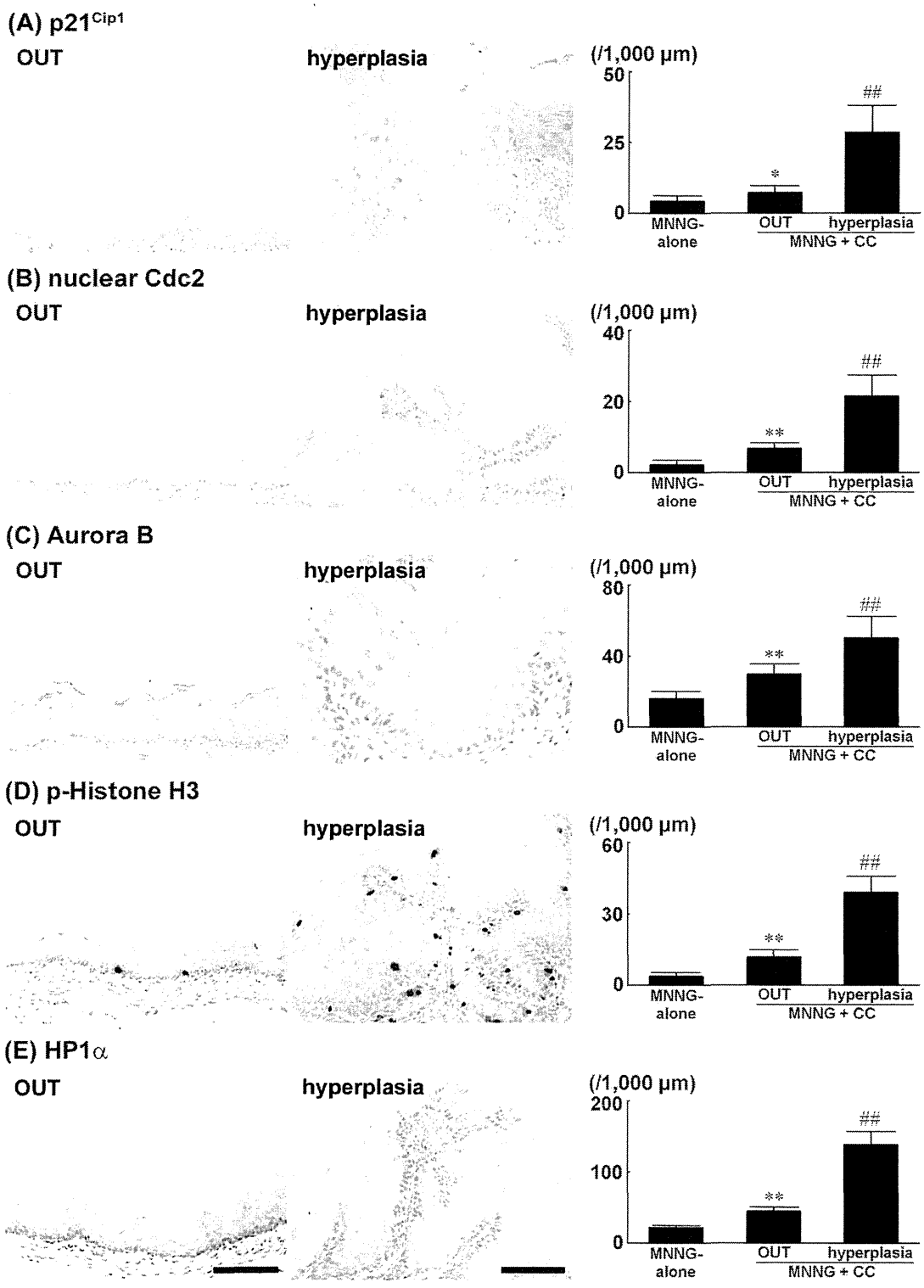

Fig. 21. Distribution of Ki-67^{+}, p21^{Cip1+}, nuclear Cdc2^{+}, Aurora B^{+}, p-Histone H3^{+} and HP1α^{+} cells in early forestomach carcinogenesis. Photomicrographs show the cellular distributions of markers in hyperplasias and surrounding cells in the MNNG + CC group. The graphs show positive cells per unit muscularis mucosae length (1,000 μm) of the mucosa in the MNNG-alone group, and of surrounding mucosa (OUT) and hyperplasias in the MNNG + CC group. Values represent mean + SD. (A) Ki-67, (B) p21^{Cip1}, (C) nuclear Cdc2, (D) Aurora B, (E) p-Histone H3, and (F) HP1α. Bar = 100 μm. *,** $P < 0.05$, 0.01 vs. the MNNG-alone group (Tukey's or Steel-Dwass multiple comparison test). $^{\#\#}$ $P < 0.01$ vs. OUT in the MNNG + CC group (Tukey's or Steel-Dwass multiple comparison test).

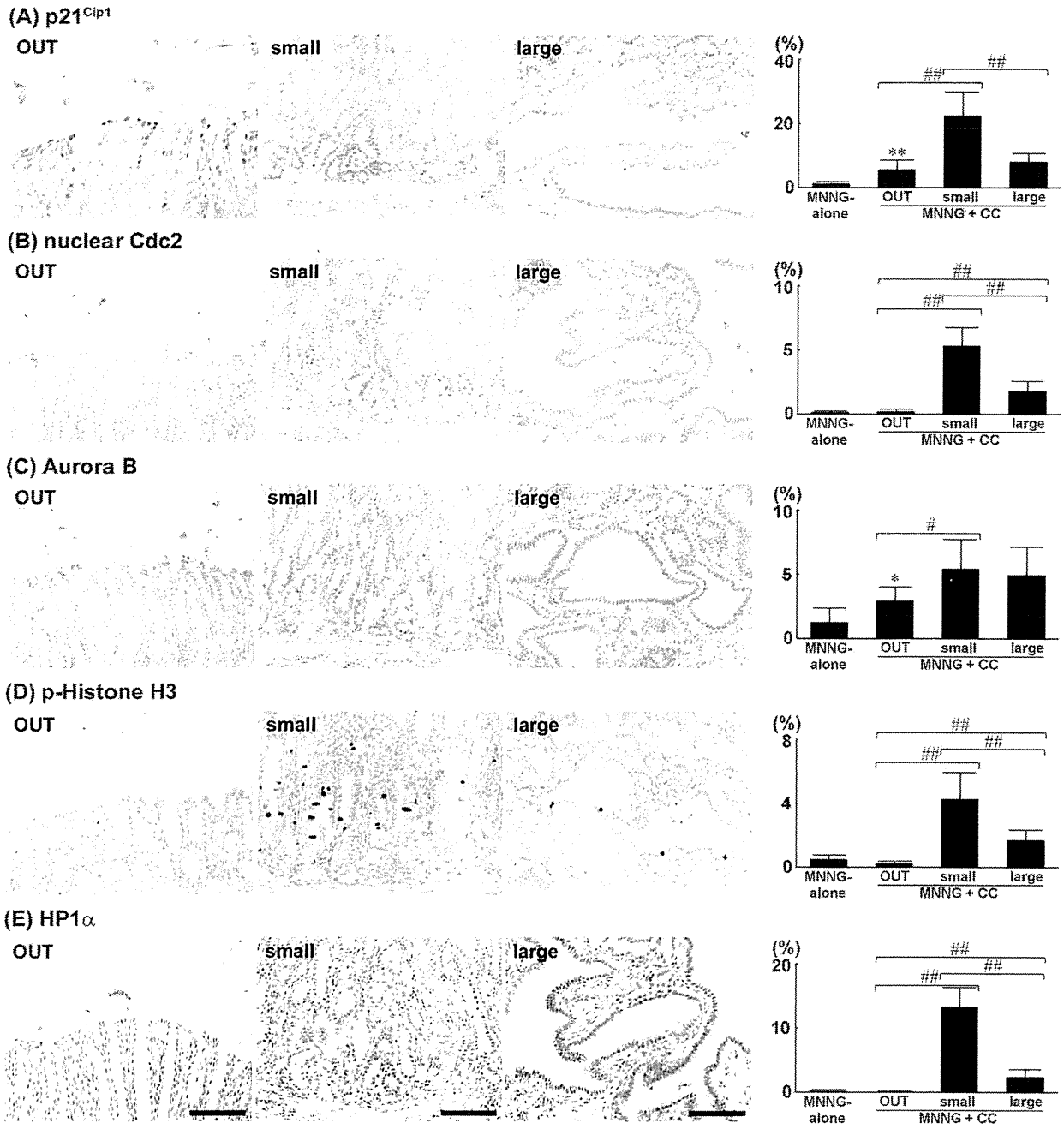

Fig. 22. Distribution of Ki-67^{+}, p21^{Cip1+}, nuclear Cdc2^{+}, Aurora B^{+}, p-Histone H3^{+} and HP1α^{+} cells in early glandular stomach carcinogenesis. Photomicrographs show the cellular distributions of markers in small hyperplastic foci, large hyperplastic foci and surrounding glandular epithelial cells in the MNNG + CC group. The graphs show positive cell ratios (%) of epithelial cells of the pyloric gland epithelia in the MNNG-alone group, and of surrounding glandular epithelial cells (OUT), and in small and large hyperplastic foci in the MNNG + CC group. Values represent mean + SD. (A) Ki-67, (B) p21^{Cip1}, (C) nuclear Cdc2, (D) Aurora B, (E) p-Histone H3, and (F) HP1α. Bar = 100 μm. *,** $P < 0.05$, 0.01 vs. the MNNG-alone group (Tukey's or Steel-Dwass multiple comparison test). $^{\#,\#\#}$ $P < 0.05$, 0.01 vs. between the groups for comparison (Tukey's or Steel-Dwass multiple comparison test).

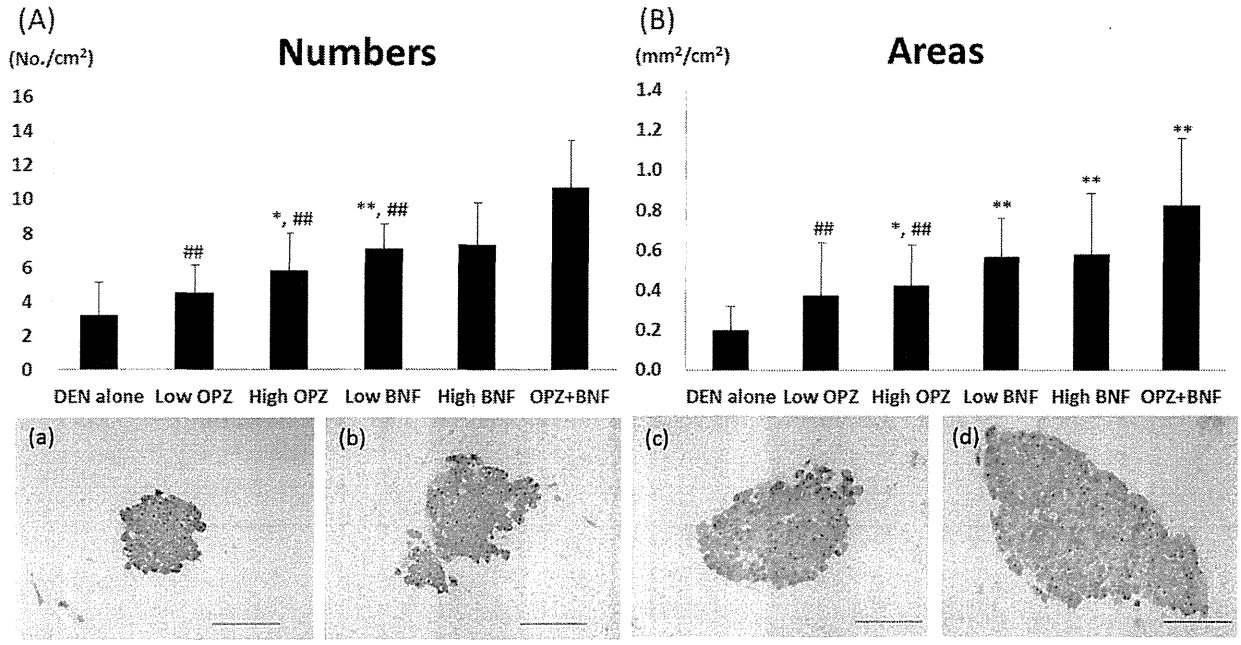

Fig. 23.

The number and area of GST-P positive foci in rats given OPZ and/or BNF after DEN initiation. Each bar shows the number (A) and area (B) of GST-P positive foci in the liver of rats given DEN alone (DEN alone), 138 mg/kg OPZ (Low OPZ), 276 mg/kg OPZ (High OPZ), 0.125% BNF (Low BNF), 0.25% BNF (High BNF) or 138 mg/kg OPZ+0.125% BNF (OPZ+BNF). Each photograph shows mean + SD of the GST-P positive foci in the liver of the DEN alone group (a), Low OPZ group (b), Low BNF group (c) and OPZ+BNF group (d).

*, ** significantly different from the DEN alone group at $p<0.05$ or $p<0.01$, respectively.

$^{\#\#}$ significantly different from the OPZ+BNF group at $p<0.01$. Original magnification: ×200 (bar: 200 μm).

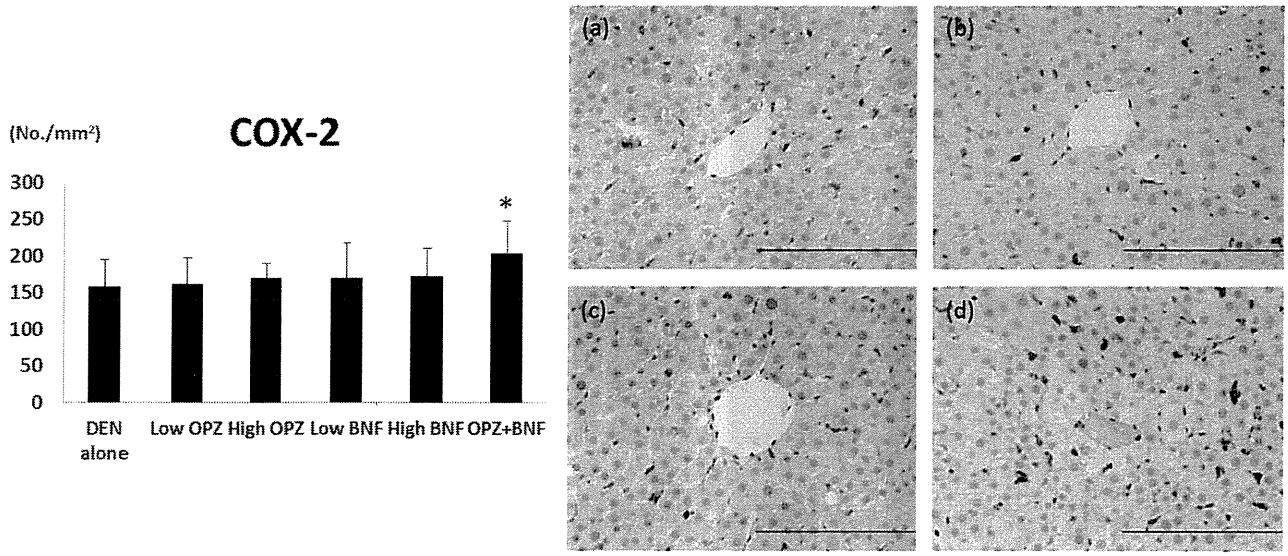

Fig. 24. Immunohistochemical photographs of COX-2 and the number of COX-2 positive cells in the liver of rats given OPZ and/or BNF after DEN initiation

Each photograph shows COX-2-positive cells in the liver of the DEN alone group (a), Low OPZ group (b), Low BNF group (c), and OPZ+ BNF group (d). Original magnification: ×100 (bar: 100 μm). The bar shows mean ± SD of the number of COX-2 positive cells in each group.

*, ** significantly different from the DEN alone group at $p<0.05$.

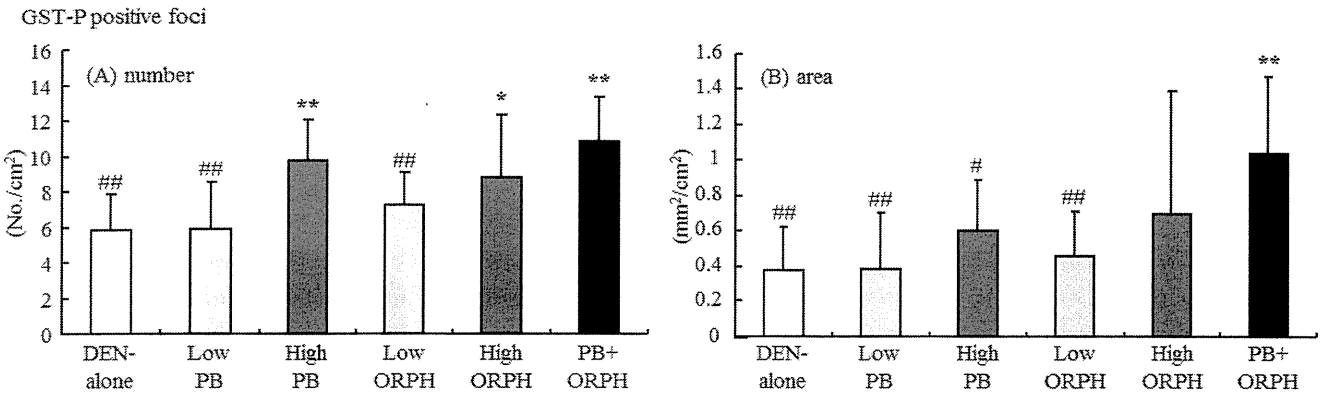

Fig. 25. Effects of PB and/or ORPH treatment on GST-P positive foci in the livers of rats given PB and/or ORPH for 6 weeks after DEN initiation. The number of GST-P positive foci in each group. Columns represent the mean + SD. (B) The area of GST-P positive foci in each group.

*, ** significantly different from the DEN-alone group (Dunnett's test or Steel test) at $p < 0.05$ or $p < 0.01$, respectively.

#, ## significantly different from the PB+ORPH group (Dunnett's test or Steel test) at $p < 0.05$ or $p < 0.01$, respectively.

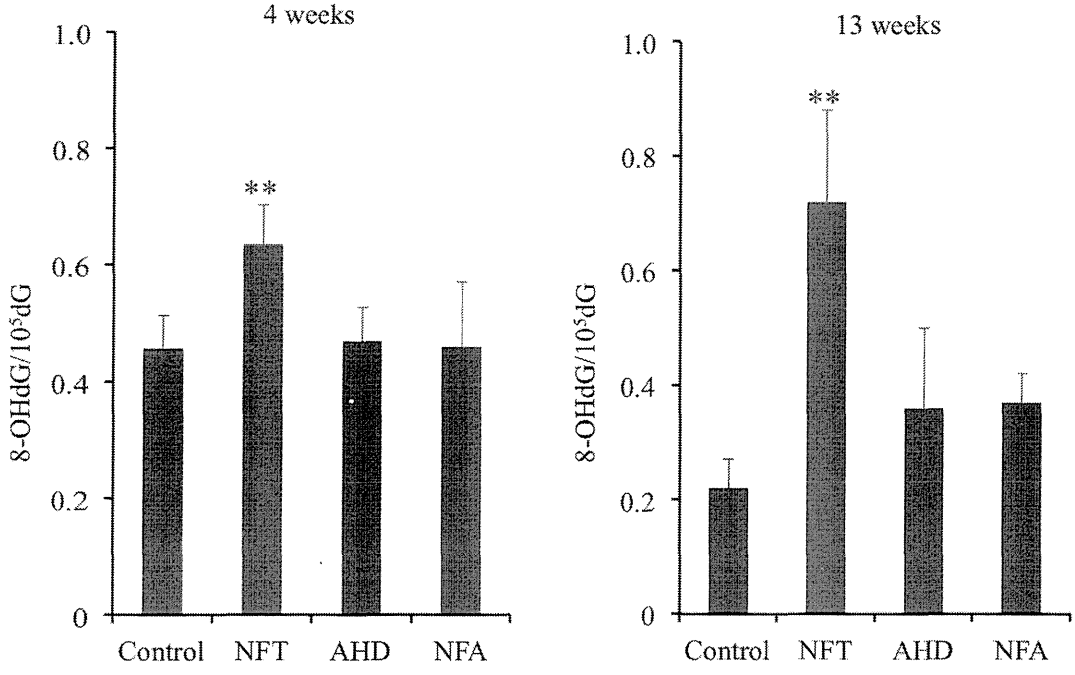

Fig. 26.
8-OHdG levels in the kidneys of male F344 *gpt* delta rats given NFT, AHD or NFA. Values are means ±SD.
**: significantly different from the control group at $p<0.01$.

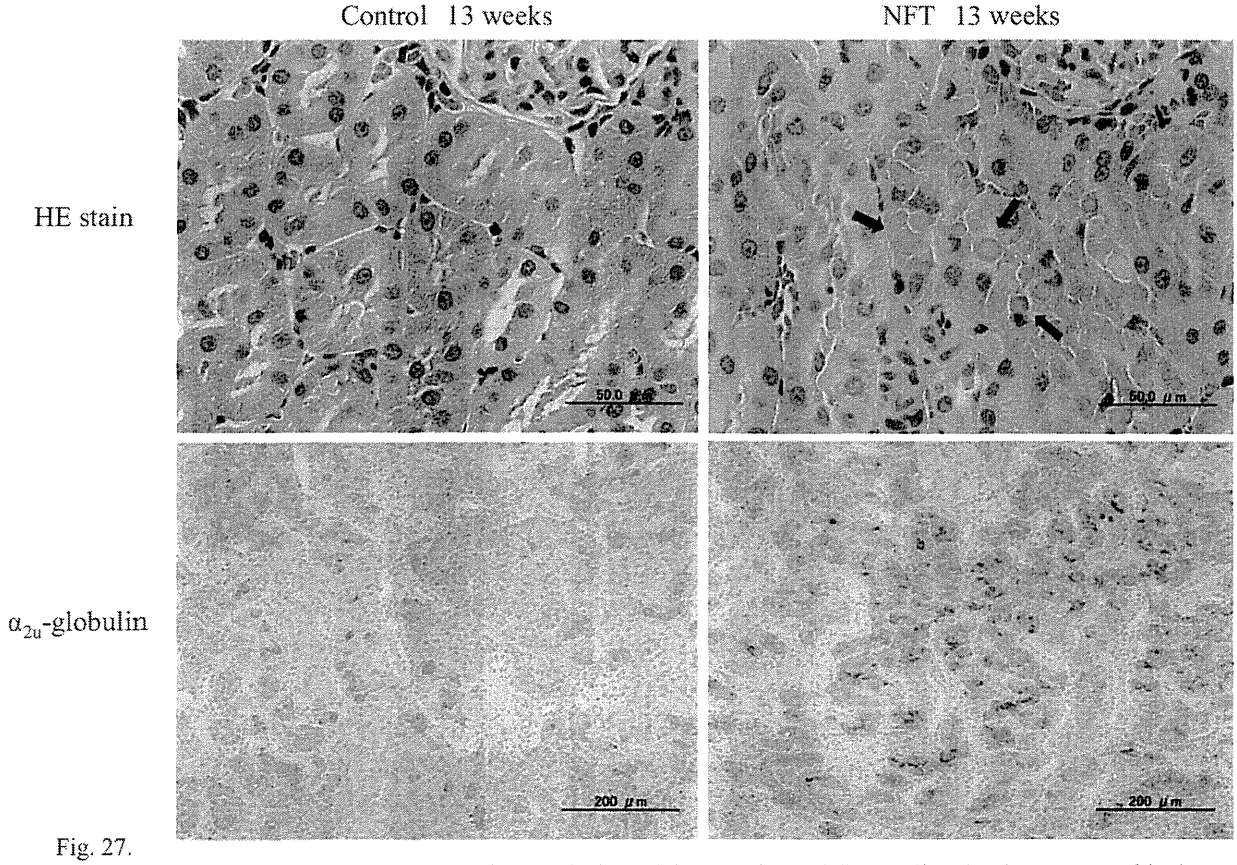

Fig. 27.
Histopathological features in the kidneys of male F344 *gpt* delta rats given NFT. Hyaline droplets were positively stained by α_{2u}-globulin immunostaining.

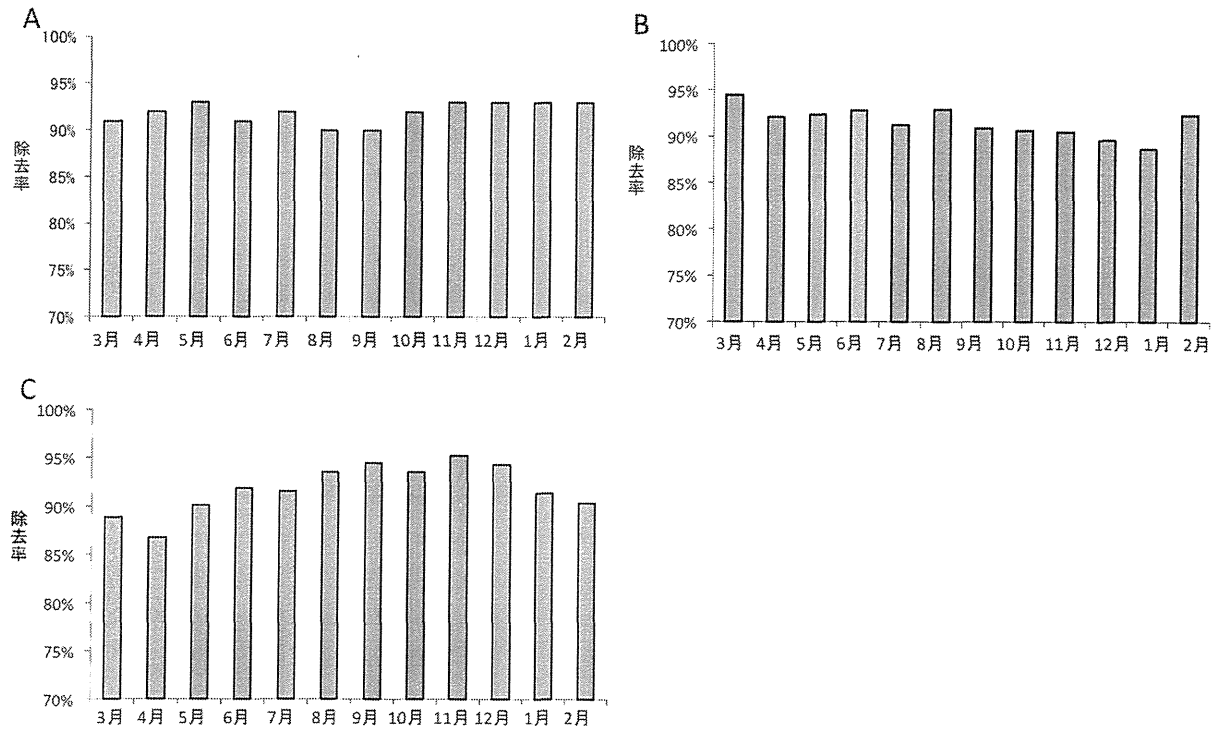

Fig. 28 背根神経節の月別除去率 A: 2010年3月～2011年2月; B: 2011年3月～2012年2月; C: 2012年3月～2013年2月

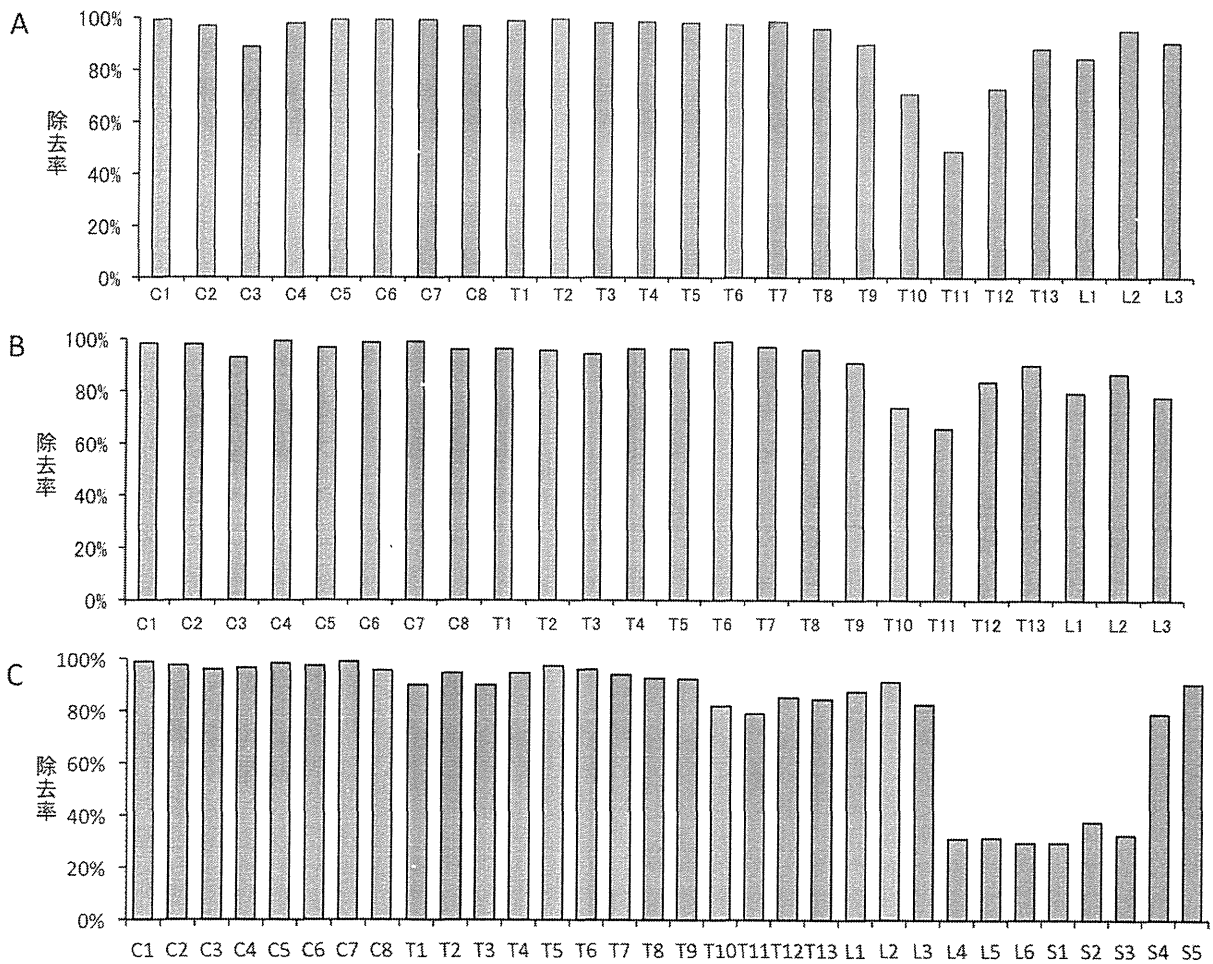

Fig. 29 背根神経節の部位除去率 A: 2010年3月～2011年2月; B: 2011年3月～2012年2月; C: 2012年3月～2013年2月

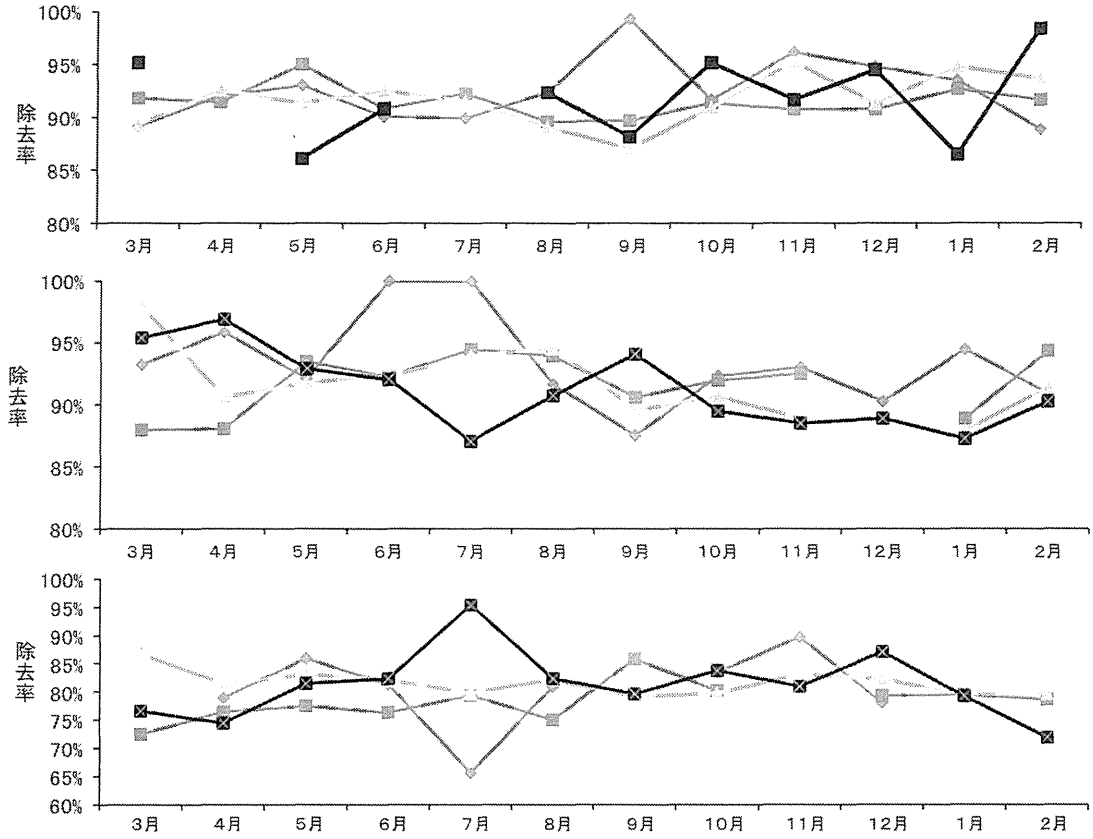

Fig. 30 牛品種別の背根神経節除去率の推移A: 2010年3月～2011年2月; B: 2011年3月～2012年2月; C: 2012年3月～2013年2月

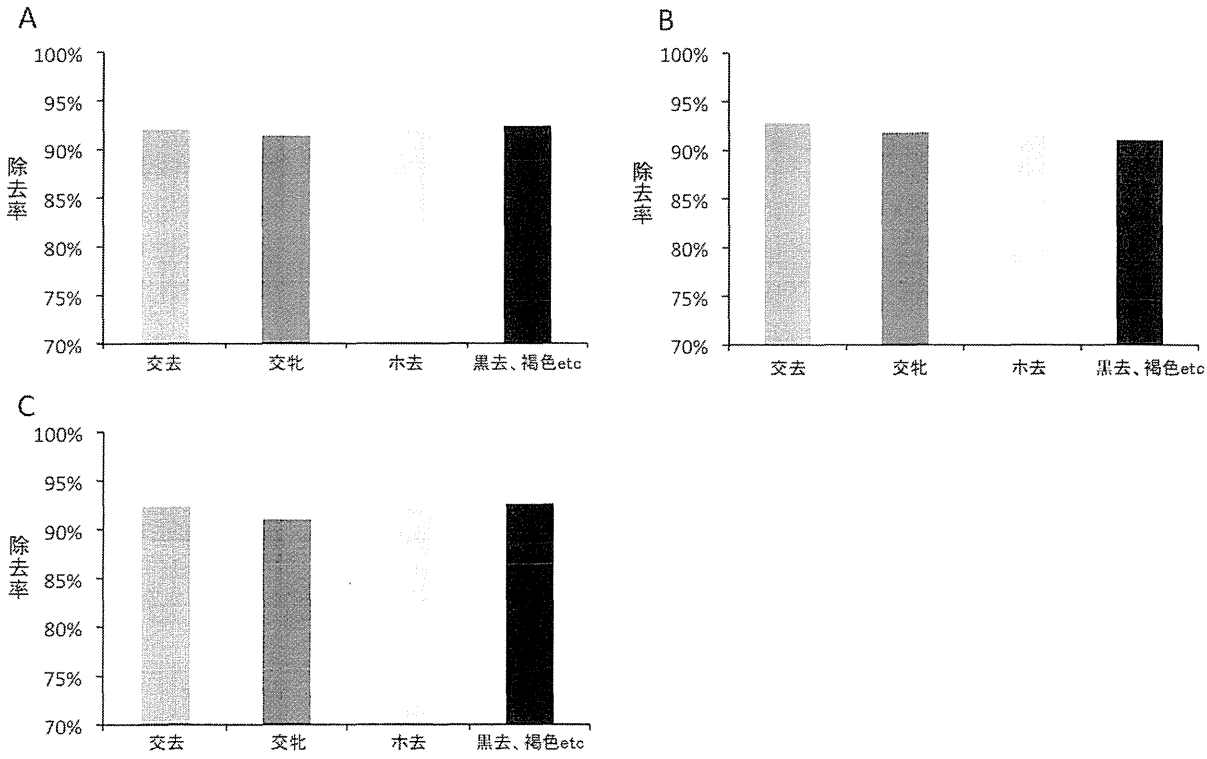

Fig.31 背根神経節の月別除去率 A: 2010年3月～2011年2月; B: 2011年3月～2012年2月; C: 2012年3月～2013年2月